International Journal of Robotics and Control Systems
Vol. 4, No. 2, 2024, pp. 941-957
ISSN 2775-2658
http://pubs2.ascee.org/index.php/ijrcs

Adaptive Load Frequency Control in Microgrids Considering PV Sources and EVs Impacts: Applications of Hybrid Sine Cosine Optimizer and Balloon Effect Identifier Algorithms

Ahmed Tawfik Hassan [a,1], Fahd A. Banakhr [b,2], Mohamed Metwally Mahmoud [a,3,*], Mohamed I. Mosaad [b,4], Asmaa Fawzy Rashwan [a,5], Mohamed Roshdi Mosa [a,6], Mahmoud M. Hussein [a,c,7], Tarek Hassan Mohamed [a,8]

[a] Electrical Engineering Department, Faculty of Energy Engineering, Aswan University, Aswan 81528, Egypt
[b] Department of Electrical and Electronics Engineering, Yanbu Industrial College, Yanbu Industrial City 41912, Saudi Arabia
[c] Department of Communications Technology Engineering, Technical College, Imam Ja'afar Al-Sadiq University, Baghdad, 10053, Iraq
[1] ahmedthhhh@gmail.com; [2] banakhrf@RCJY.EDU.SA; [3] Metwally_M@aswu.edu.eg; [4] m_i_mosaad@hotmail.com; [5] rashwan_asmaa@yahoo.com; [6] Mohamed.roshdy@yahoo.com; [7] mahmoud_hussein@aswu.edu.eg; [8] tarekhie@yahoo.com
* Corresponding Author

ARTICLE INFO

Article history
Received May 05, 2024
Revised June 07, 2024
Accepted June 14, 2024

Keywords
LFC;
Microgrid;
Hybrid Sine Cosine and Balloon Effect Method;
Uncertainties;
Green Energy

ABSTRACT

The negative impacts of microgrids (µGs) on the load frequency highlight the importance of implementing a robust, efficient, and adaptable controller to ensure stability. This work introduces an adaptive load frequency control (LFC) for an isolated µG that includes a PV system and electric vehicles (EVs), which have a significant impact on frequency. This control utilizes a combination of sine cosine optimization (SCO) and balloon effect identifier (BEI) algorithms. The controller presented in this work transforms the LFC process into an optimization problem that is highly compatible with various random situations encountered in the control process. The suggested control method is a novel approach by utilizing SCO+BEI for adaptive LFC application, resulting in a highly efficient response. The effectiveness of the proposed adaptive controller is assessed under the conditions of 17 MW variable load, system parameters uncertainties, and installed PV systems of 6 MW. MATLAB / Simulink package is rummage-sale as a digital test environment. According to simulation results, the proposed adaptive controller succeeds in regulating the frequency and power of an islanded µG. To measure the efficiency of the proposed control scheme, a comparison between other control techniques (such as adaptive controller using Jaya+BEI and classical integral controller) is done. The findings of the studied scenarios assured that the not compulsory control method using (SCO+BEI) has an obvious superiority over other control methods in terms of frequency solidity in case of random load instabilities and parameter uncertainties. Finally, it can be said that the proposed controller can better ensure the safe operation of the µGs.

1. Introduction

The worldwide use of energy has grown annually since the dawn of industrialization, and issues with the climate throughout the world have had a significant influence on both the natural world and human culture. As a result, many nations have established zero emissions objectives [1], [2]. Renewable sources of energy (REOS) must be added to the electrical supply side, like solar (PV) and wind power, in order to alter the energy architecture. These sources can be used on-site by a microgrid (μG) with multi-energy complementing capabilities, enabling quick growth and implementation. In the meantime, a μG is a crucial tool for upcoming grid sophisticated healing oneself, user-side interactions, and demand-side responses, which encourages the usage of numerous components, including electric vehicles, to reduce fluctuations [3], [4]. Thus, investigation into the stability control of μGs is essential due to dispersed power generation's high unpredictability.

REOS are clean, economical, and easy to use, but their disadvantage is lack of continuity due to weather changes, so the focus was on storing it [5]-[7]. Research on the impact of integrating REOS on frequency in μGs is currently a popular subject of study, alongside control approaches. [8], [9]. The presence of the REOS beside the traditional energy systems leads to changes in the voltage frequency in the distribution systems. The mechanical and electrical connections between different types of power systems especially between fossil power systems and renewable power supported its safety and security. However, it needs more optimal sophisticated technology. Compared with μGs it has a lot of difficulties in installation. It was very important for adding modified and adjusted load frequency control (LFC) to a classical integrated control unit which is usually used in LFC applications [10], [11]. For these reasons, actual solutions must be required to maintain the characteristics of frequency deviations and voltage variations to stay within an optimum value [12], [13]. A comparison of the cost, reliability, and consistency of the models has been done with the information in [14], where replicas have been described built on the archetypal design and communication structure.

LFCs' primary function is to eliminate frequency (F) deviations and then alter the F's system in response to unanticipated disturbances or changes. It is well known that synchronous generators' stored rotor inertia energy plays a key role in preserving the system's stability in the presence of faults. The F of power systems (PSs) need to be stabilized and regulated in this direction. REOS are now being quickly integrated into conventional PSs. Plans for the future indicate that REOSs will be important globally. Due to their low stored inertia, these REOSs minimize the PS's overall inertia [15]-[17].

To combat the detrimental impacts of REOS on the stability of PSs, investigations have been done in recent years. Many control strategies have been addressed to boost the system's stability [15], [18], [19]. In [20], the damping properties and inertial rapid responses under faults were enhanced by changing the points of operation of the wind turbine (WT) from the maximum power point (MPP) to the virtual inertia control (VIC) curves with respect to the F deviation. The concept of droop control for VIC on WTs was presented in [21] in order to enhance the dynamic reactions of the PS. The grid-side converter was used in [22] to service F and voltage adjustment. A VIC utilizing the $H\infty$ technique was suggested in [23] to enhance the F reliability of an μG. To enhance system dynamic reactions, wind generators were used as a virtual machine (VM) in [11]. Adjustable VIC was suggested via updating the parameters of the VIC to improve F stability [24]. In [25], a bang-bang control strategy-based VM was developed, and a small signal model analyses the system's stability. In order to realize an adaptable system for adjusting the inertia variable of the VM, an adaptive strategy was provided to achieve the necessary responsiveness [26]. These approaches' primary flaw is that they are reliant on the precision of the model's mathematics.

Ref [27], provides sophisticated frequency control for controlling μGs to lessen F and power variations. The stability and management of the μG, which was autonomous by a fuzzy regulator and comprised several REOS [28]. Ref. [29] examined the state feedback approach for determining system eigenvalues and modifying the controller's settings to analyze the stability of a hybrid μG. Ref., [30] presents an inertial sampling method-based μG frequency control with a supplementary control. In [31], the LFC of a multi-zone PS with a wind generator was investigated, while [32] presents a study of back-to-back converter-equipped μGs. The differential evolutionary technique for LFC of μGs with storage units was suggested in [33], where the absence of a controller design was carried out by taking uncertainties into account.

Utilizing several optimization techniques, the adaptive control issue is demonstrated. As illustrated in [34], similar methods are used to precisely adjust the strictures of fuzzy and neural regulators. The managed variable's error rate determines the object function (OF) in certain circumstances. As mentioned in [35], the adaptive controller's parameters can also be adjusted directly utilizing optimization techniques. But, the OF was built, for example, utilizing time-based reply physical appearance like rising time (T_r), settling time (T_s), and overshoot (M_P): $J_{min} = \sum(M_P + T_s + T_r)$.

A disadvantage of this technique, especially for time-variant systems, is that $M_P, T_s \; and \; T_r$ consist of operations in the mechanism variables' basic levels. To solve this problem, a BE modification has recently been proposed [34]. The balloon effect (BE) aims to have the OF communicate with the new stricture values and other structure changes. In summary, fundamental algorithm techniques may be used to change the resistor constraints in a range of practical and business requests, such as temperature regulators, motor regulators, etc.

Several articles have suggested optimization strategies to increase the F stability of μGs. The main issue with these strategies can be regarded as their non-robust functioning. A novel technique for adjusting the gains of controllers is sine cosine optimization (SCO) and proves its effectiveness in optimizing PI-fractional order-PID controller of hybrid μG system F response. Furthermore, a multi-layer perceptron is also used with SCO, and its outcomes are compared to grey wolf and whale optimizers. The new hybrid (SCO+BE) is supposed in this paper to address this problem and make the technique more sensitive to instabilities and parameter variations. In order to optimize F regulation for variable loads and parameters in smart μG, this paper recommends using the SCO+BE. Diesel generators, load, and PV frame the considered system. The impact of F fluctuations carried out via implementing arbitrary loads and ROESs is examined concerning the wished-for SCO+BE method. Additionally, it is compared with Jaya and conventional integral techniques to demonstrate its sturdiness and accuracy. Nonetheless, there is a growing tendency in the installation of controlled loads in isolated grids, including EVs and HP [36], [37]. In [36], the smart μG system's frequency regulation is achieved by installing HPs and EVs in residential areas. This paper discussed the effect of connecting the EV units on the studied microgrid's frequency during the system difficulties such as penetration resulting from renewable sources such as PV sources.

These are the primary distinguishing qualities of this work:

- An online adaptive LFC is presented using the SCO+BE method which is nursed from the output terminals of the open-loop basic TF of μG.
- The effectiveness of a SCO+BE optimizer-adjusted integral controller in adaptable frequency is investigated.
- The studied comparative performance of the suggested technique proves it is better than the conventional I, adaptive using Jaya algorithms and adaptive controller using SCO.
- Besides adaptive hybrid (SCO+BE) controller, controlled loads such as EVs can cooperate in enhancing the total system frequency.

The rest of the paper is organized as follows: Section 2 describes the islanded single area μG dynamic model and presents its configuration and modeling. Sections 3 and 4 discuss the standard SCO and the modified (SCO+BE) algorithm. Section 5 bargains the results and discussions of the wished-for controlled schemes. Finally, Section 6 accomplishes the effort.

2. Description, Modeling, and Investigations on the Studied System

To examine the F behavior of the system, F modeling of µGs built around the block schematic connections of each generation source is provided. The most efficient F control approach in the case of PV is then sequentially outlined utilizing an appropriate adaptation of the I controller using the SCO+BE technique. The F error is chosen in the optimization OF such that the variations in F are dampened over time to lower the settings of the time domain in the form of the ISTSE-OF. To increase the F stability of µGs, supplies will be used in µGs. Additionally, the suggested regulator has been used in the µG and its settings will be optimally adjusted so that any F variations brought on by disruptions like overload can be effectively dampened and the µG will continue to operate

2.1. µG -LFC

Generating power must be balanced with the general ingesting of energy and losses for the µG to operate properly. The F and power allotted to the devices may be distorted periodically since the point of operation of the system is continually shifting. On the µG, these variations can have unintended consequences. LFC is one of the most significant issues in the development and execution of µGs, alongside automated control of output, and it ought to be carefully taken into account during the design process. The following can be used to sum up the main goals to regulate the LFC of the µG: Guarantee that the change in F is zero in the case of island mode, Lower variations in F when altering the situation from grid linking mode to island mode and vice versa, precise monitoring of loads and disruptions, Minimize the duration of settling time and determine the highest possible overshoot\undershoot value when departing in F [38].

The µG is by nature nonlinear and time-variable. The F-reaction of the µG to minor load changes can be studied and analyzed using the structure's linearized system. The oscillations of the µG-F reaction vary from a limited seconds up to a limited minutes and they are significantly sluggish than the rotor's voltage and angle subtleties. As a result, a far more simplified model than those now utilized for studying and modeling different kinds of dynamics is employed to simulate the frequency behavior of the PS concerning disturbances. The majority of investigations use a first-order (FO) pre-phase transfer function (TF) to represent REOS to examine the F behavior of µGs. The µG-F response model and a few REOS are discussed in the paragraphs that follow [38].

2.2. Power System Dynamic Model

A µG-PS's structure is displayed in Fig. 1. The next equations explain the suggested µG-PS's dynamic framework. [39]; the whole load-generator dynamic relationship between the supply error (ΔP_d - ΔP_L) and the F deviation (Δf) is written as:

$$\Delta f = \left(\frac{1}{M}\right).\Delta Pd - \left(\frac{1}{M}\right).\Delta PL - \left(\frac{D}{M}\right).\Delta f \tag{1}$$

The diesel generator' dynamic power (DGP) can be expressed as:

$$\Delta Pd = \left(\frac{1}{Td}\right).\Delta Pg - \left(\frac{1}{Td}\right).\Delta Pd \tag{2}$$

The governor's dynamic (GD) power is:

$$\Delta Pg = \left(\frac{1}{Tg}\right).\Delta Pc - \left(\frac{1}{R.Td}\right).\Delta f - \left(\frac{1}{Tg}\right).\Delta Pg \tag{3}$$

Where ΔP_g is the GD output, ΔP_d is the DGP change, Δf is the F change, ΔP_L is the load change, ΔP_c is the added control action, M is the comparable inertia constant, D is the correspondent damping coefficient, R is the speed drop typical, T_g is the GD time constant, T_d is the turbine time constant, and (Δf, ΔP_d, ΔP_g) equal to ($\frac{df}{dt}$, $\frac{dPd}{dt}$, $\frac{dPg}{dt}$), respectively.

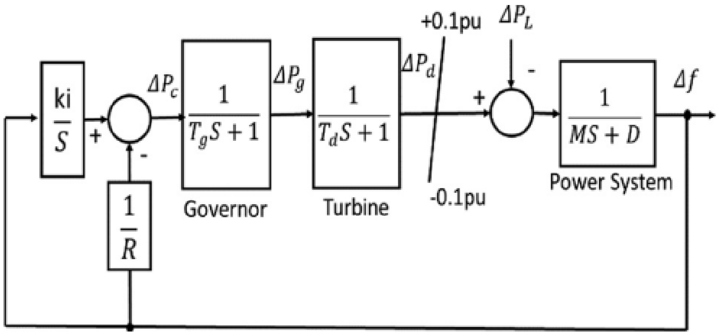

Fig. 1. The µG-PS model

2.3. Diesel Generator (DsG) Modeling

Turbine and governor systems are components found in DsG. The generator, turbine, and governor's FO models are provided by (4)-(6) [27]:

$$G_{DsG} = \frac{K_{DsG}}{1 + ST_{DsG}} = \frac{\Delta P_{DsG}}{\Delta f} \tag{4}$$

$$G_{Turbine}(s) = \frac{1}{ST} \tag{5}$$

$$G_g(s) = \frac{1}{1 + ST_{gi}} \tag{6}$$

where (K_{DsG}, T_{DsG}), and (T_{gi}, and T) are the gain and time constant of the TF of the DsG, and the time constant of the governor and turbine of the DsG.

2.4. PV Modeling

Equations (7) and (8) specify the F model and the resulting power of the studied PV [40].

$$P_{PV} = \emptyset S\eta\{1 - 0.005(T_a + 25)\} \tag{7}$$

$$G_{PV} = \frac{K_{PV}}{1 + ST_{PV}} = \frac{\Delta P_{PV}}{\emptyset} \tag{8}$$

where S, and (K_{PV} and T_{PV}) is the surface area of the PV (m^2), the gain and time constant of the PV−TF.

3. The Proposed Hybrid Technique

3.1. The Sine Cosine Optimization (SCO)

Element of the cluster clever optimization process is iterated, as part of the traditional SCO analysis and assumption. Serial examines the method's first solution established, which is a set of several arbitrary choices. Set the answer via arbitrary iteration. ultimately finds the best answer that satisfies the conditions. SCO uses an iterative process to accomplish an arbitrary search inside the solving space; however, it is unable to provide the best solution in a single iteration. Finding the best answer can be significantly enhanced by selecting a starting value and a sufficient number of repetitions. The prior methods' repetition approaches are summarized as follows: in the worldwide exploration stage, an enormous random number of repetitions is applied to obtain a superior solution established for searching unexplored areas in the outcome space; in the localization of the platform, an insufficient arbitrarily disruption is applied to the substance establish to completely search the surrounding area of the present solution. This simplifies the iteration process of the prior methods into two phases. An incremental formula realizing the two threads expressions for worldwide exploration and community growth is constructed based on the cyclical fragility of the trigonometric function. The response pool is updated and disturbances are placed on it using the concise refresh recurrent formula. Furthermore, additional methods for computation that evolve. The capability of the randomized optimization algorithms to find solutions through both local and global searching is what determines their capacity. Many scholars have been working on improving SCO to boost its efficacy even more ever since its initial proposal [41], [42]. The pseudo-code of SCO is fully discussed in [42].

By using old-style SCO, eq (9) shows the place to keep informed:

$$X_i^{t+1} = \begin{cases} X_i^t + r_1 \times \sin(r_2) \times \left|r_3 P_i^t - X_i^t\right|, r_4 < 0.5 \\ X_i^t + r_1 \times \cos(r_2) \times \left|r_3 P_i^t - X_i^t\right|, r_4 \geq 0.5 \end{cases} \tag{9}$$

Here, $r_2 \in [0, 2\pi]$, is an arbitrary mutable. r_3 is a causal variable. r_4 is used to select diverse search paths, sine or cosine, according to different random values in Eq. (9). Pi is the OF solution. r_1 is an integer that, to equalize the computational search procedure, is reduced from m to 0 during the iterations. The display looks like this:

$$r_1(i) = m \times (1 - \frac{1}{i_{max}}) \tag{10}$$

where i is the present iteration, i_{max} is the total number of iterations, and m > 0.

3.2. Proposed Optimization

3.2.1. Improved Position-Updating Equation

Traditional SCO algorithms have better convergence and accuracy in optimization problems. However, the presence of absolute value and trigonometric functions in the position updating equations leads to a nonlinear search path. This can make it challenging to find the global optimum in complex problems. Additionally, the conjunction rate of outdated SCO decreases as the number of scopes grows. To address these issues, an improved SCO algorithm is proposed that incorporates a linear search path inspired by PSO. This new approach recalls the random assortment of sine and cosine while providing a more effective search trajectory [43].

The technical description of the converged factor is altered by variables and the two distinct path features, which cancel out the absolute value. The following is the path-searching phrase:

$$X_i^{k+1} = \begin{cases} r_1 X_i^k + C_1 \sin(r_2)\ \left(P_{best-i}^k - X_i^k\right) + C_2 \sin(r_2)\ \left(E_{best}^k - X_i^k\right), r_3 < 0.5 \\ r_1 X_i^k + C_1 \cos(r_2)\ \left(P_{best-i}^k - X_i^k\right) + C_2 \cos(r_2)\ \left(E_{best}^k - X_i^k\right), r_3 < 0.5 \end{cases} \tag{11}$$

where Pi is the best remedy, X_i is the exact spot of the current best remedy, and k is the count of current iterations. The enhanced SCO enhances search in challenging optimization problems by combining a linear search path with the original path, denoted by the parameter r1, which is also known as the convergence factor. The convergence factor denoted as r1, balances prospection and development in the search. By incorporating the linear path, the algorithm reduces oscillations and improves search speed, resulting in efficient discovery of the global optimum. Just as Fig. 2 depicts. According to [44], curve A finding the global optimum is necessary, as indicated by point A in Fig. 3. An experimental restriction is acquainted with the search track to expand search exactness by utilizing knowledge and information from previous iterations. This parameter has been successfully applied in antenna pattern optimization, achieving good results [44]. The final expression for the search path is as follows:

$$X_i^{k+1} = \begin{cases} r_1 X_i^k + C_1 \sin(r_2)\ \left(P_{best-i}^k - X_i^k\right) + C_2 \sin(r_2)\ \left(E_{best}^k - X_i^k\right), r_3 < 0.5 \\ r_1 X_i^k + C_1 \cos(r_2)\ \left(P_{best-i}^k - X_i^k\right) + C_2 \cos(r_2)\ \left(E_{best}^k - X_i^k\right), r_3 < 0.5 \end{cases} \tag{12}$$

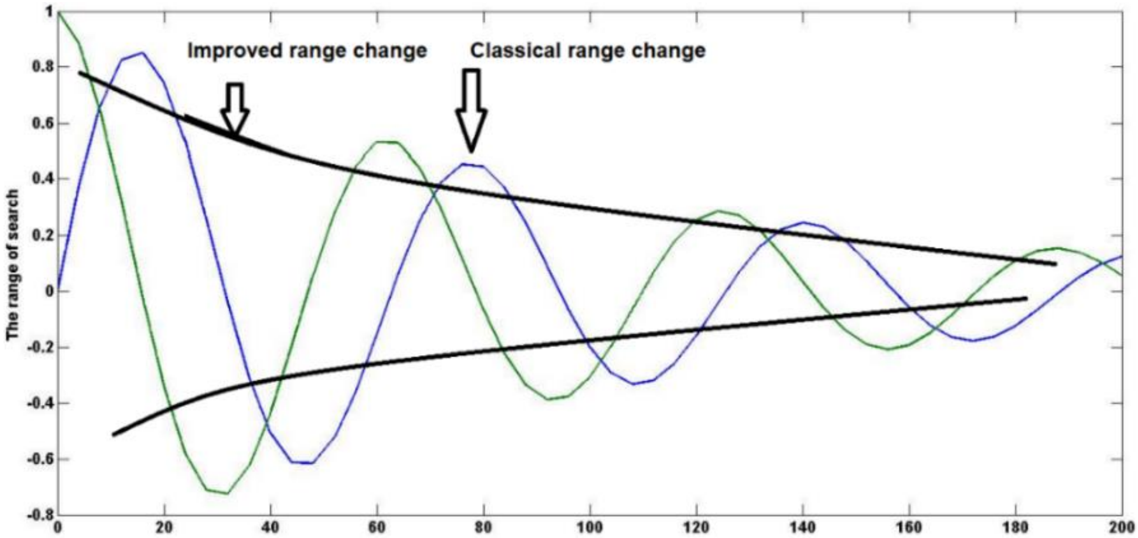

Fig. 2. The enhanced and traditional range switching

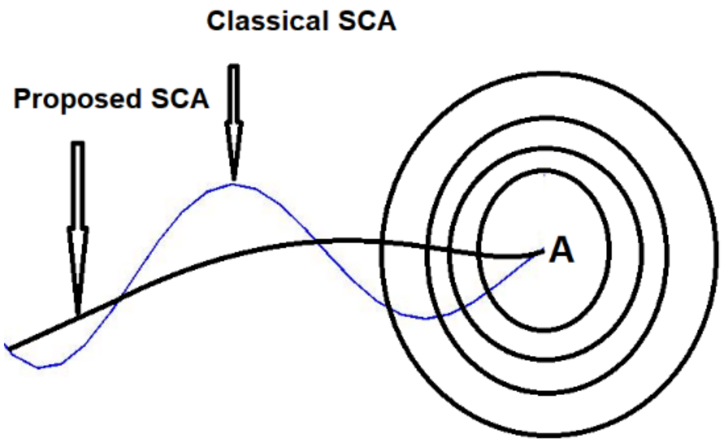

Fig. 3. Comparing several search routes

In (12), r_1 is the convergence factor, r2 ∈ [0, π/2], and the selection of either the sine or cosine path is controlled by a random number called r3. Constants C_1 and C_2 can be changed to reflect real-world issues. The experimental variable from the preceding iteration is denoted by E. Pi is the best possible answer. The optimization method's search becomes more effective with the addition of a straight path. The universal optimal can be located more quickly and with greater certainty by introducing empirical parameters under the joint constraints of E and P. These enhancements will make the algorithm more suitable for challenging optimization issues.

3.2.2. Enhanced Convergence Factor (CF)

Furthermore, this paper modifies the established list of associated variables. In addition, it is crucial to specify a CF with superior algorithmic performance. r_1 is stated below in (13):

$$r_1 = r_{max} - (r_{max} - r_{min})\frac{t}{T} \tag{13}$$

The CF is defined using the constants r_{max} and r_{min}, which can be adjusted according to the specific problem. By modifying the parameter m, the flexibility of the CF is increased. This allows for adaptation to various optimization scenarios. Initially, a greater CF aids in refining the universal search fitness. As the iteration progresses, the CF gradually decreases to a smaller value (SV). The prime of this SV and the rate of decrease contribute to refining the ultimate result of the SCO. The proposed modified SCO algorithm's flowchart is shown in Fig. 4.

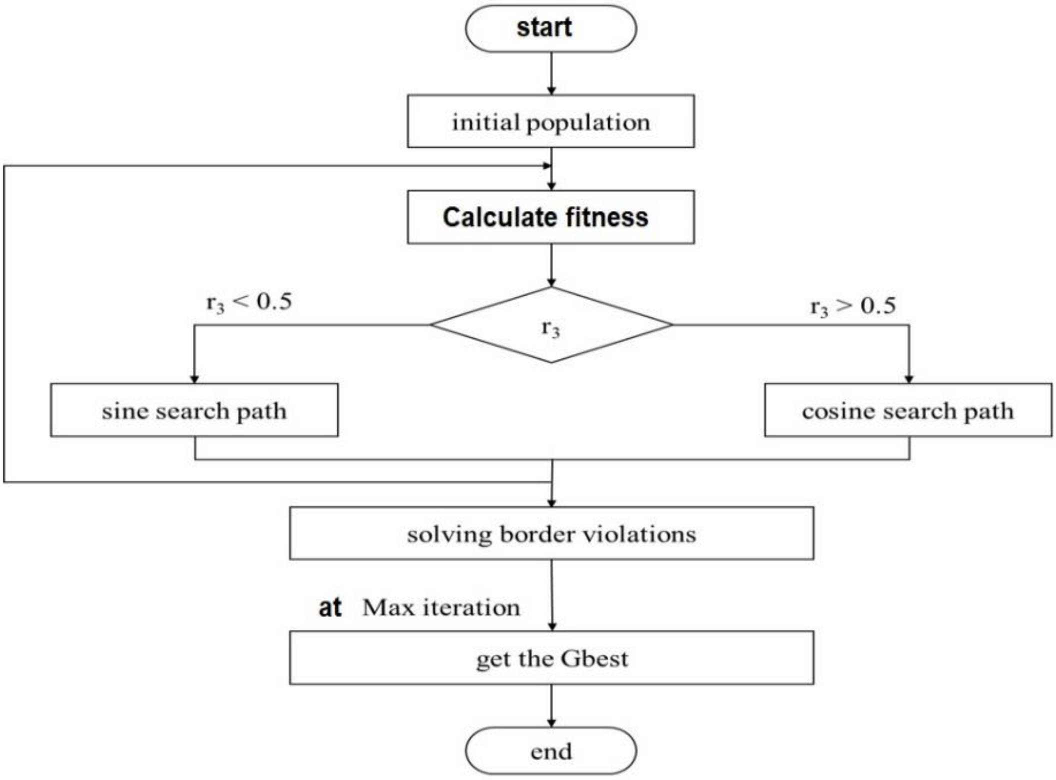

Fig. 4. The flowchart of the modified SCO

3.2.3. BE Identifier Technique

The BE, similar to the effect of air on a balloon's size, refers to the impact of system challenges such as disturbances and parameter uncertainty on Gi(s). Fig. 5 illustrates how the BE identifier influences the (OF) of an optimization strategy at apiece repetition. By incorporating this technique, the optimization procedure is upgraded and better able to handle the mentioned challenges [45]. The online TF of µG for any iteration (i) will be:

$$G_i(\mathrm{s}) = \frac{Y_i(s)}{U_i(s)} \tag{14}$$

Furthermore, $\mathrm{G_i}(s)$ is a function of its previous value $G_{i-1}(s)$. AL_i Stands for a gain and $G_0(s)$ represents the nominal process transfer function.

$$\mathrm{G_i}(s) = AL_i G_{i-1}(s) \tag{15}$$

$$G_{i-1}(s) = \rho_i G_0(s) \tag{16}$$

Where

$$\rho_i = \prod_{n=1}^{i-1} AL_n \tag{17}$$

$$G_i(s) = AL_i \rho_i G_0(s) \tag{18}$$

4. SCO-Based BE Identifier

Fig. 6 illustrates a simplified µG model; it is employed to determine the restricted area's FO closed-loop system's variables.

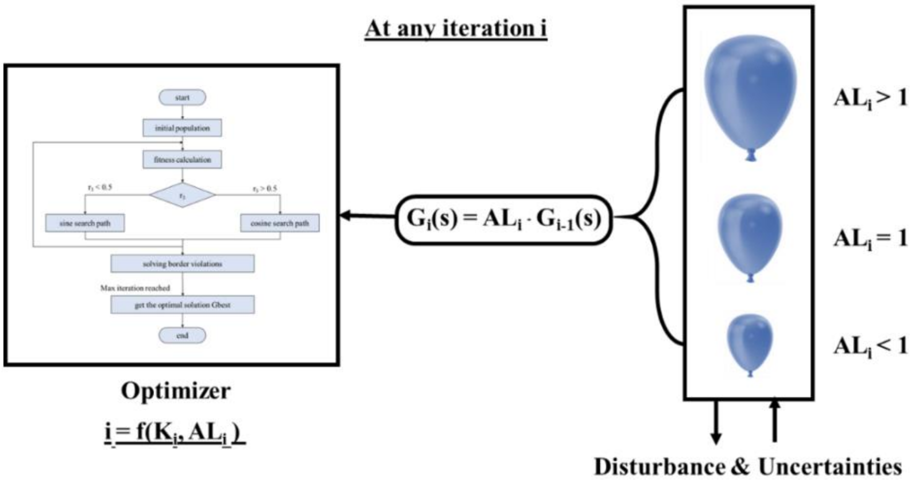

Fig. 5. An optimization strategy-based identifier for the BE [45]

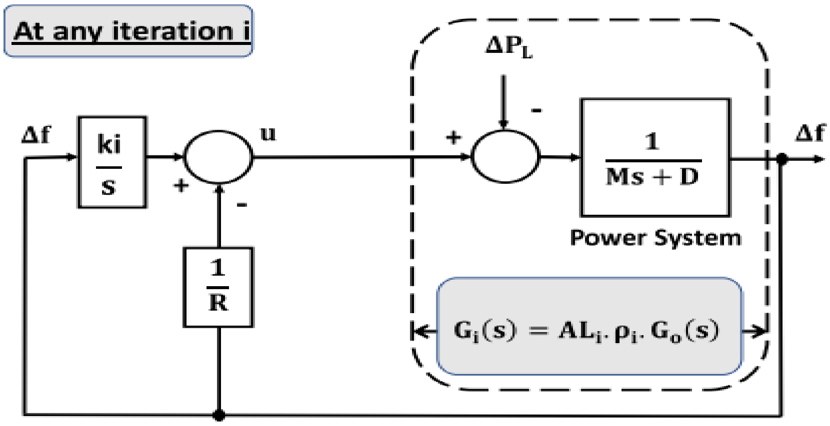

Fig. 6. Reduced model of the studied microgrid

$$\mathrm{T.F} = \frac{wn^2}{S^2 + 2\eta Wn + Wn^2} = \frac{\frac{Ki}{Mo}}{S^2 + \left(\frac{\left(Do + \frac{1}{Ro}\right)}{Mo}\right)S + \frac{Ki}{Mo}} \tag{19}$$

where D_o, R_o, and M_o are the nominal values of D, R, and M, respectively

$$\omega_n = \sqrt{\mathrm{Ki/Mo}}, \eta = \frac{\frac{(Do+\frac{1}{Ro})}{Mo}}{2\omega_n} \tag{20}$$

$$T_r = \frac{\pi - \sqrt{(1-\eta^2)}}{\omega_n\sqrt{(1-\eta^2)}}, T_s = \frac{4}{\eta\omega_n}, M_P = e^{\frac{-\pi\,\eta}{\sqrt{(1-\eta^2)}}} \tag{21}$$

This is the SCO-based BE identifier's OF.

$$J = min \sum(T_r + T_s + M_P) \tag{22}$$

This means that the OF (J) is a function of AL_i and k_i to address the system challenges.

5. Results and Discussion

In this section, a digital simulation platform has been used to study a 20 MW isolated μG with nominal parameters listed in Table 1. In addition, Fig. 7 illustrates a power flowchart for the studied μG, the following four cases have been used to study the μG with the suggested controller compared with other controllers in varied situations.

Table 1. Parameters of the studied μG

Parameter	D	H=(M/2)	R	T_g	T_d
Unit	(Pu/Hz)	(pu. sec)	(Hz/Pu)	(sec)	(sec)
Value	0.015	0.08335	3	0.08	0.4

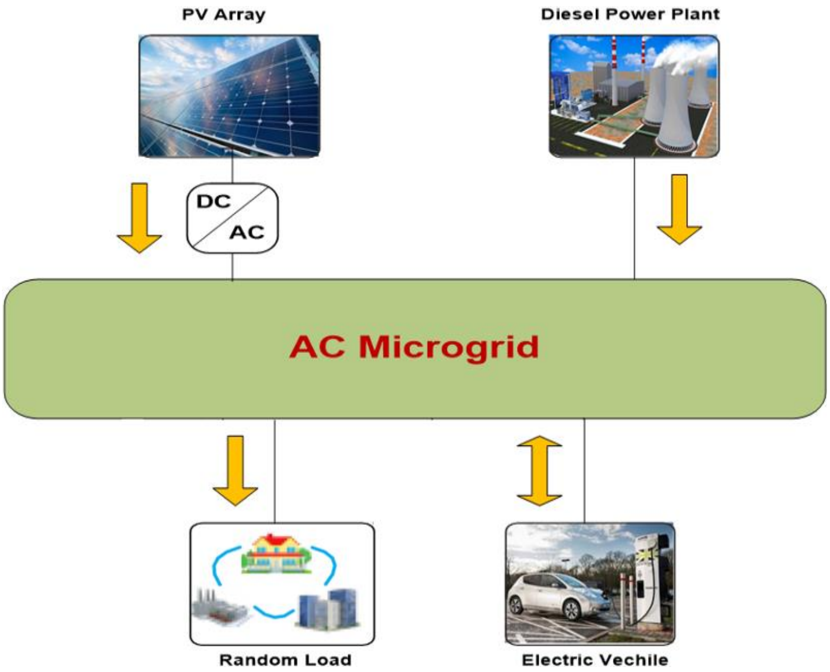

Fig. 7. The power flowchart for the studied μG

5.1. Case 1: System Performance Under a Step Load

In this situation, the system's performance under a step load demand has been tested with nominal specifications. The load in this example increases from 0 pu to 0.02 pu at t = 3 sec. We consider both the governor dead band GD and the turbine GRC. The GD is 0.05 pu, and the turbine GRC is 10% per minute [46]. By contrasting this control approach with SCO+BE with the fixed parameter integral controller I, the adaptive one using only SCO, and the adaptive controller utilizing the Jaya optimization (JO) method (with details listed in [36]), the effectiveness of this control method is determined. Table 2 contains a list of the SCO's defined parameters. Table 3 lists the defined variables of the used JO. Fig. 8-a depicts the change in system F deviation when an integral controller with fixed parameters, an adaptive controller using the conventional JO approach published in [47], and a suggested controller are used. While Fig. 8-b illustrates the DsG power change in the same case, according to Fig. 8, In comparison to the value produced utilizing the conventional controller, the system with JO and SCO methods M_p, T_{ss}, and T_r has been reduced to around 20% and SCO + BE is the best.

Table 2. Data of SCO

Maximum iteration (IT max)	100
Population size (k)	5
Convergence constant (a)	2

Table 3. Data of JO

Population size (k)	5
Number of generations (*i*)	50
Number of design variables (m)	2

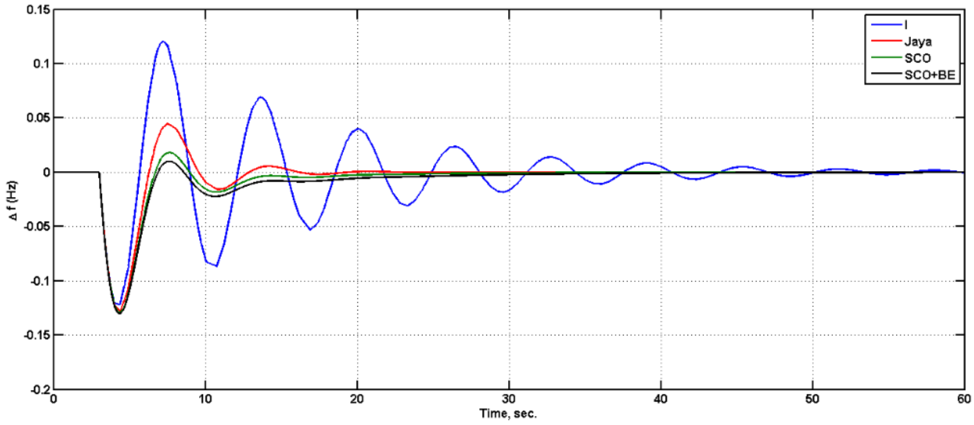

(a)

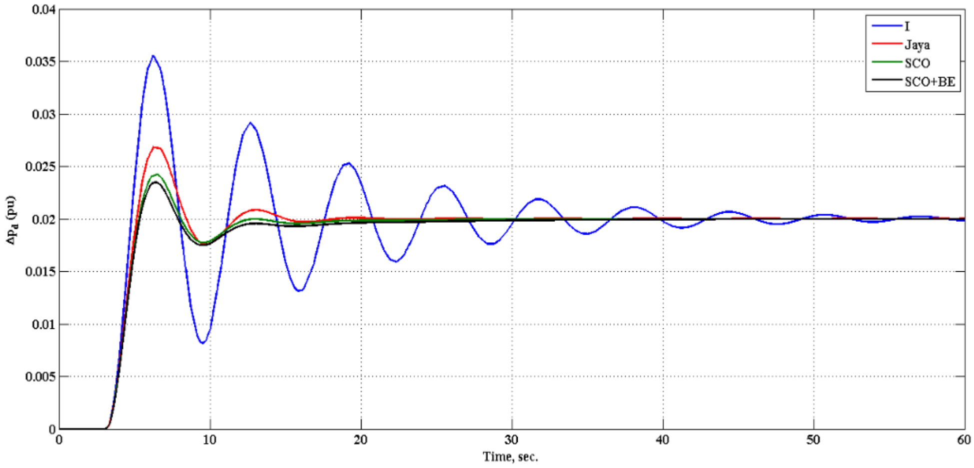

(b)

Fig. 8. System response for case 1, a) frequency deviation and b) diesel power deviation

5.2. Case 2: Impact of Changing Parameters on the Investigated μG

A system with a suggested control strategy was looked at when parameters varied. D is raised by 100%, and the time constants T_d and T_g are increased by a factor of 150%. Fig. 9 and Fig. 10 show a comparison of the system response obtained with the four different controllers (fixed I, tuned by JO, tuned by SCO, and tuned by SCO+BE). The F response of the fixed parameter I controller is not acceptable, but systems with I adjusted by JO, SCO, and SCO+BE can successfully manage these issues, according to this graph. Additionally, the system with the suggested SCO+BE method provides high performance and the fastest response.

5.3. Case 3: Impacts of PV and Variable Load on the Investigated μG

The system has been tested under various operating circumstances. Testing is done with a 17 MW variable load, taking into account the system's nominal characteristics and adding a 6 MW PV to the μG as a second source of power, as shown in Fig. 11, Fig. 12 shows that the suggested technique has the greatest performance in terms of F response for the system with the proposed controller. In comparison to the conventional I and I tuned by JO, tuned by SCO approaches, this figure demonstrates the advantages of the recommended online tuned controller utilizing the (SCO+ BE) methodology.

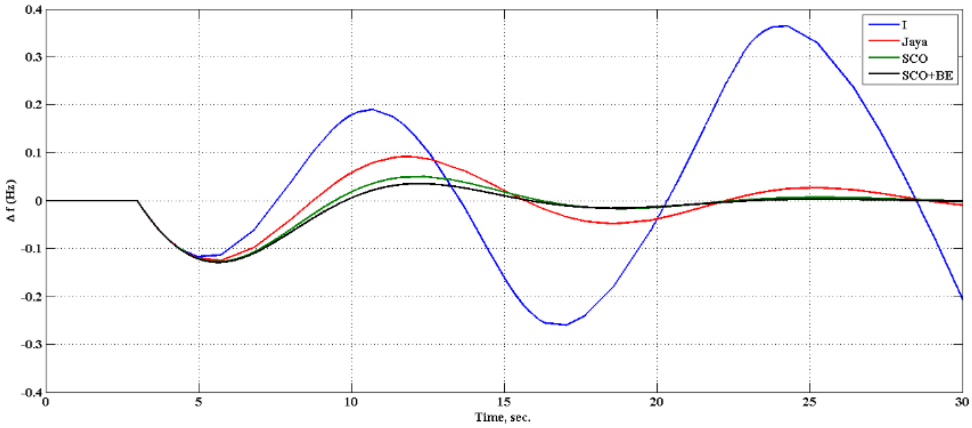

Fig. 9. System response for case 2, frequency deviation

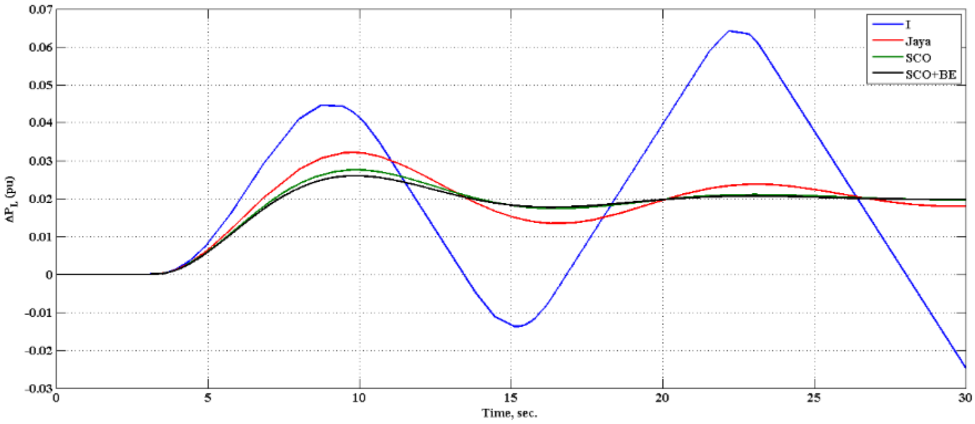

Fig. 10. System response for case 2, diesel power deviation

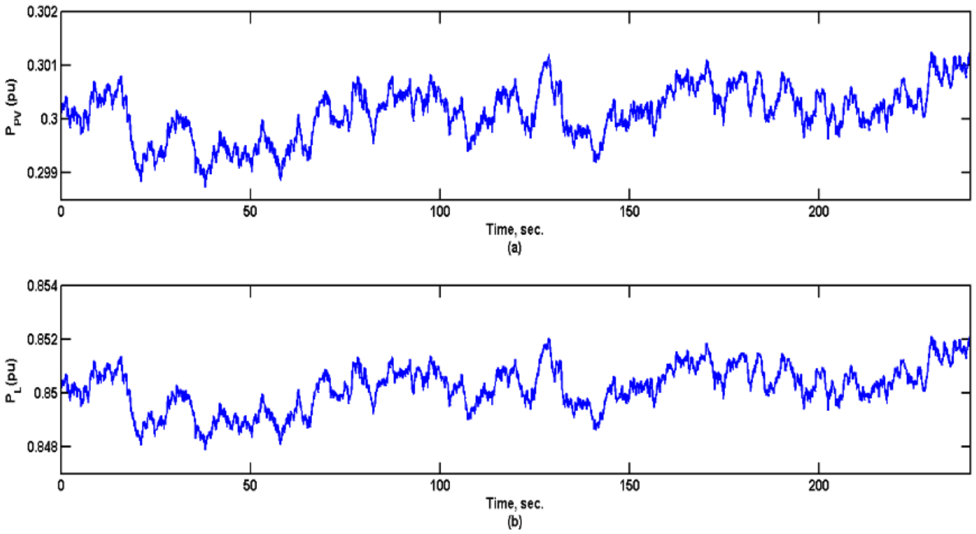

Fig. 11. PV power and random load

5.4. Case 4: Impact of EVs on the Investigated μG

Finally, the effect of merging the EVs to the proposed μG is discussed. The details of the used EVs are shown in Appendix A. Fig. 13 shows the repetition of case 3 but in the presence of 2 units of EVs (1.19 MW/unit) while Fig. 14 shows the EV participation power change. From Fig. 14, it is noticeable that: besides the proposed SCO+BE controller, the presence of EVs can positively affect the total system frequency in such cases of penetrations.

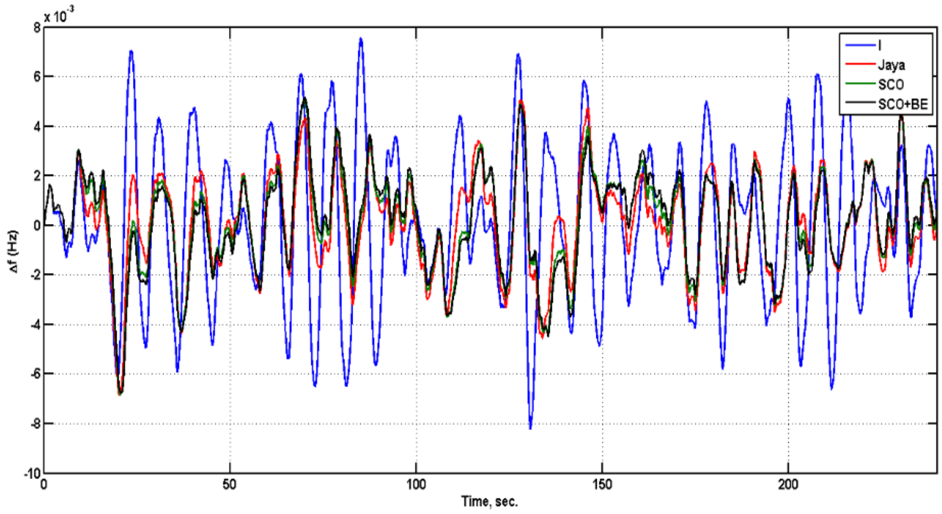

Fig. 12. System response for case 3, frequency deviation

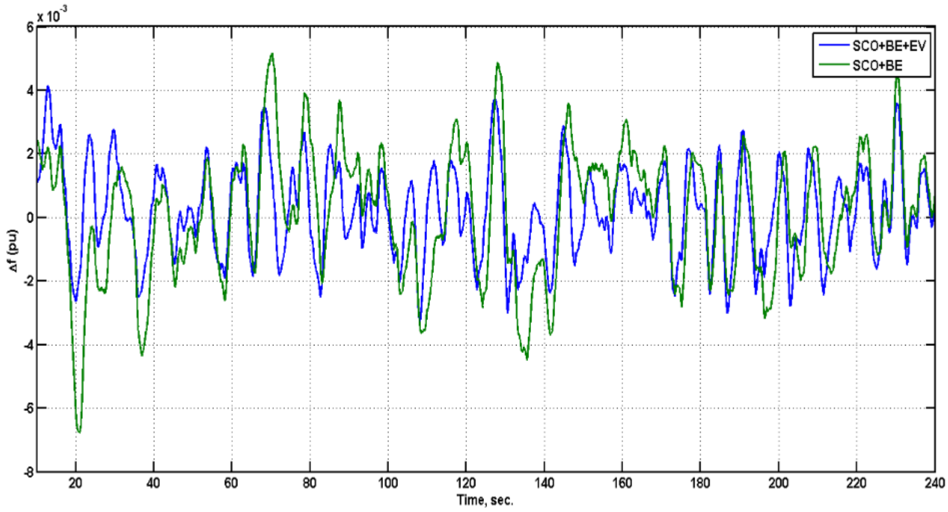

Fig. 13. System response for case 4, frequency deviation

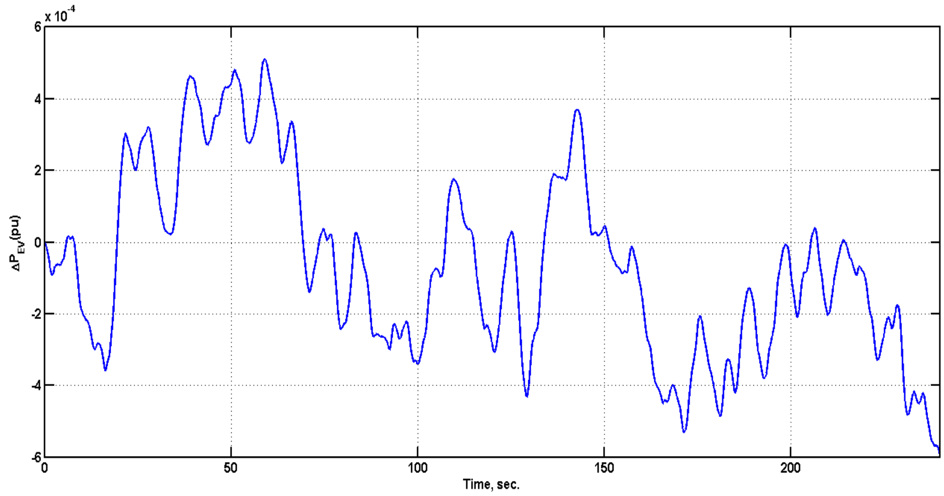

Fig. 14. EV participation power change

6. Conclusion

An adaptive LFC method based on SCO and (SCO+BE) is proposed in this paper to address F regulation in the presence of disturbances and parameter uncertainties. A digital simulation is conducted to evaluate the proposed control method under the influence of random demand loads and variable PV power generation. The results are compared with other controllers, including the fixed integrated controller, JO, and SCO controller on the μG, and thoroughly analyzed. The system with the proposed SCO+BE can give the best frequency response compared with other controllers (Mp decreased by 80% and settling time minimized by 90% compared with conventional I controller). In addition, systems with SCO+BE, SCO, and JO can keep stability in case of changes in the system parameters while systems with conventional I controllers cannot. It is recommended to use a controller with gains that can be tuned using SCO + BE to solve LFC problems and reduce system oscillations. In addition, the presence of controlled loads such as EVs has affected positively the system performances, such as minimizing the system frequency deviations.

Author Contribution: All authors contributed equally to the main contributor to this paper. All authors read and approved the final paper.

Data Availability: The data used to support the findings of this study are available at reasonable request from the corresponding author.

Conflicts of Interest: The authors declare that they have no conflicts of interest.

Funding: This work has no external funding.

Appendix

Fig. 15 illustrates the dynamic model of the electric vehicle aggregated model where T_{EV} is the time constant of the unit, and U_{EV} is the control signal of the controller that is fed by the system frequency deviation as input signal. In this work, $T_{EV} = 0.28$, $P_{EV\text{-rated}} = 1.19$ pu, and the controller of the EVs unit is a robust H_2/H_∞ method with details mentioned in [36].

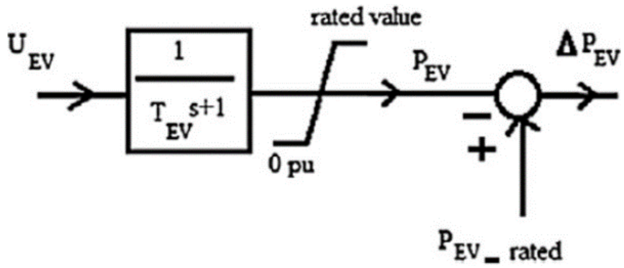

Fig. 15. The dynamic model of the EV unit

List of abbreviations

REOS: Renewable sources of energy
VIC: Virtual inertia control
LFC: Load frequency control
MPP: Maximum power point
PI-FOPID: PI-fractional order PID
VM: Virtual machine
TF: Transfer function
F: Frequency
μG: Microgrid
PV: Solar
BE: Balloon effect
PS: power system
SCO: Sine Cosine optimization.
I: Integral
FO: First order
DsG : Diesel Generator

References

[1] G. Yanagawa and H. Aki, “Grid Flexibility Provision by Optimization of Fast-Charging Demand of Battery Electric Vehicles,” *IEEE Transactions on Smart Grid*, vol. 14, no. 3, pp. 2202-2213, 2023, https://doi.org/10.1109/TSG.2022.3219403.

[2] N. Benalia *et al*., "Enhancing electric vehicle charging performance through series-series topology resonance-coupled wireless power transfer," *PLoS One*, vol. 19, no. 3, p. e0300550, 2024, https://doi.org/10.1371/journal.pone.0300550.

[3] H. Bevrani, F. Daneshfar and T. Hiyama, "A New Intelligent Agent-Based AGC Design With Real-Time Application," *IEEE Transactions on Systems, Man, and Cybernetics, Part C (Applications and Reviews)*, vol. 42, no. 6, pp. 994-1002, 2012, https://doi.org/10.1109/TSMCC.2011.2175916.

[4] M. Awad *et al*., "A review of water electrolysis for green hydrogen generation considering PV/wind/hybrid/hydropower/geothermal/tidal and wave/biogas energy systems, economic analysis, and its application," *Alexandria Engineering Journal*, vol. 87, pp. 213-239, 2024, https://doi.org/10.1016/j.aej.2023.12.032.

[5] A. Smolarz *et al*., "Increasing Technical Efficiency of Renewable Energy Sources in Power Systems," *Energies*, vol. 16, no. 6, p. 2828, 2023, https://doi.org/10.3390/en16062828.

[6] R. Kassem *et al*., "A Techno-Economic-Environmental Feasibility Study of Residential Solar Photovoltaic / Biomass Power Generation for Rural Electrification : A Real Case Study," *Sustainability*, vol. 16, no. 5, p. 2036, 2024, https://doi.org/10.3390/su16052036.

[7] M. M. Mahmoud, "Improved current control loops in wind side converter with the support of wild horse optimizer for enhancing the dynamic performance of PMSG-based wind generation system," *International Journal of Modelling and Simulation*, vol. 43, no. 6, pp. 952-966, 2023, https://doi.org/10.1080/02286203.2022.2139128.

[8] G. Shahgholian, "A brief review on microgrids: Operation, applications, modeling, and control," *International Transactions on Electrical Energy Systems*, vol. 31, no. 6, p. e12885, 2021, https://doi.org/10.1002/2050-7038.12885.

[9] A. M. Ewias *et al*., "Advanced load frequency control of microgrid using a bat algorithm supported by a balloon effect identifier in the presence of photovoltaic power source," *PLoS One*, vol. 18, no. 10, p. e0293246, 2023, https://doi.org/10.1371/journal.pone.0293246.

[10] D. Saha, N. Bazmohammadi, J. C. Vasquez, and J. M. Guerrero, "Multiple Microgrids: A Review of Architectures and Operation and Control Strategies," *Energies*, vol. 16, no. 2, p. 600, 2023, https://doi.org/10.3390/en16020600.

[11] T. Kerdphol, F. S. Rahman, Y. Mitani, M. Watanabe and S. K. Küfeoğlu, "Robust Virtual Inertia Control of an Islanded Microgrid Considering High Penetration of Renewable Energy," *IEEE Access*, vol. 6, pp. 625-636, 2018, https://doi.org/10.1109/ACCESS.2017.2773486.

[12] H. Abubakr, J. C. Vasquez, T. Hassan Mohamed, and J. M. Guerrero, "The concept of direct adaptive control for improving voltage and frequency regulation loops in several power system applications," *International Journal of Electrical Power & Energy Systems*, vol. 140, p. 108068, 2022, https://doi.org/10.1016/j.ijepes.2022.108068.

[13] M. M. Hussein, T. H. Mohamed, M. M. Mahmoud, M. Aljohania, M. I. Mosaad, and A. M. Hassan, "Regulation of multi-area power system load frequency in presence of V2G scheme," *PLoS One*, vol. 18, no. 9, p. e0291463, 2023, https://doi.org/10.1371/journal.pone.0291463.

[14] M. Z. Kreishan and A. F. Zobaa, "Optimal allocation and operation of droop-controlled islanded microgrids: A review," *Energies*, vol. 14, no. 15, p. 4653, 2021, https://doi.org/10.3390/en14154653.

[15] M. A. El-Hameed, M. M. Elkholy, and A. A. El-Fergany, "Efficient frequency regulation in highly penetrated power systems by renewable energy sources using stochastic fractal optimiser," *IET Renewable Power Generation*, vol. 13, no. 12, pp. 2174-2183, 2019, https://doi.org/10.1049/iet-rpg.2019.0186.

[16] J. Liu, Y. Miura and T. Ise, "Comparison of Dynamic Characteristics Between Virtual Synchronous Generator and Droop Control in Inverter-Based Distributed Generators," *IEEE Transactions on Power Electronics*, vol. 31, no. 5, pp. 3600-3611, 2016, https://doi.org/10.1109/TPEL.2015.2465852.

[17] A. M. Ewais, A. M. Elnoby, T. H. Mohamed, M. M. Mahmoud, Y. Qudaih, and A. M. Hassan, "Adaptive frequency control in smart microgrid using controlled loads supported by real-time implementation," *PLoS One*, vol. 18, no. 4, p. e0283561, 2023, https://doi.org/10.1371/journal.pone.0283561.

[18] C. Chen, K. Zhang, J. Geng, K. Yuan, Z. Yang, and L. Li, "Multiobjective-based optimal allocation scheme for load frequency control," *International Transactions on Electrical Energy System*, vol. 27, no. 7, p. e2334, 2017, https://doi.org/10.1002/etep.2334.

[19] M. H. Fini and M. E. H. Golshan, "Determining optimal virtual inertia and frequency control parameters to preserve the frequency stability in islanded microgrids with high penetration of renewables," *Electric Power Systems Research*, vol. 154, pp. 13-22, 2018, https://doi.org/10.1016/j.epsr.2017.08.007.

[20] Y. Li, Z. Xu and K. P. Wong, "Advanced Control Strategies of PMSG-Based Wind Turbines for System Inertia Support," *IEEE Transactions on Power Systems*, vol. 32, no. 4, pp. 3027-3037, 2017, https://doi.org/10.1109/TPWRS.2016.2616171.

[21] H. Ye, W. Pei and Z. Qi, "Analytical Modeling of Inertial and Droop Responses From a Wind Farm for Short-Term Frequency Regulation in Power Systems," *IEEE Transactions on Power Systems*, vol. 31, no. 5, pp. 3414-3423, 2016, https://doi.org/10.1109/TPWRS.2015.2490342.

[22] K. Strunz, K. Almunem, C. Wulkow, M. Kuschke, M. Valescudero and X. Guillaud, "Enabling 100% Renewable Power Systems Through Power Electronic Grid-Forming Converter and Control: System Integration for Security, Stability, and Application to Europe," *Proceedings of the IEEE*, vol. 111, no. 7, pp. 891-915, 2023, https://doi.org/10.1109/JPROC.2022.3193374.

[23] M. Moafi, M. Marzband, M. Savaghebi, and J. M. Guerrero, "Energy management system based on fuzzy fractional order PID controller for transient stability improvement in microgrids with energy storage," *International Transactions Electrical Energy Systems*, vol. 26, no. 10, pp. 2087-2106, 2016, https://doi.org/10.1002/etep.2186.

[24] T. Kerdphol, M. Watanabe, K. Hongesombut and Y. Mitani, "Self-Adaptive Virtual Inertia Control-Based Fuzzy Logic to Improve Frequency Stability of Microgrid With High Renewable Penetration," *IEEE Access*, vol. 7, pp. 76071-76083, 2019, https://doi.org/10.1109/ACCESS.2019.2920886.

[25] J. Li, B. Wen and H. Wang, "Adaptive Virtual Inertia Control Strategy of VSG for Micro-Grid Based on Improved Bang-Bang Control Strategy," *IEEE Access*, vol. 7, pp. 39509-39514, 2019, https://doi.org/10.1109/ACCESS.2019.2904943.

[26] M. R. Ghodsi, A. Tavakoli, and A. Samanfar, "Microgrid Stability Improvement Using a Deep Neural Network Controller Based VSG," *International Transactions Electrical Energy Systems*, p. 7539173, 2022, https://doi.org/10.1155/2022/7539173.

[27] N. Mohamed, F. Aymen, Z. M. Ali, A. F. Zobaa, and S. H. E. Abdel Aleem, "Efficient power management strategy of electric vehicles based hybrid renewable energy," *Sustainability*, vol. 13, no. 13, p. 7351, 2021, https://doi.org/10.3390/su13137351.

[28] X. Li, Y. J. Song, and S. Bin Han, "Frequency control in micro-grid power system combined with electrolyzer system and fuzzy PI controller," *Journal of Power Sources*, vol. 180, no. 1, pp. 468-475, 2008, https://doi.org/10.1016/j.jpowsour.2008.01.092.

[29] M. Mahmoudi, H. Jafari and R. Jafari, "Frequency control of Micro-Grid using state feedback with integral control," *2015 20th Conference on Electrical Power Distribution Networks Conference (EPDC)*, pp. 1-6, 2015, https://doi.org/10.1109/EPDC.2015.7330464.

[30] J. Morren, S. W. H. de Haan, W. L. Kling and J. A. Ferreira, "Wind turbines emulating inertia and supporting primary frequency control," *IEEE Transactions on Power Systems*, vol. 21, no. 1, pp. 433-434, 2006, https://doi.org/10.1109/TPWRS.2005.861956.

[31] R. Ahmadi, A. Sheikholeslami, A. Nabavi Niaki, and A. Ranjbar, "Dynamic participation of doubly fed induction generators in multi-control area load frequency control," *International Transactions Electrical Energy Systems*, vol. 25, no. 7, pp. 1130-1147, 2015, https://doi.org/10.1002/etep.1891.

[32] R. Alayi, F. Zishan, M. Mohkam, S. Hoseinzadeh, S. Memon, and D. A. Garcia, "A sustainable energy distribution configuration for microgrids integrated to the national grid using back-to-back converters in a renewable power system," *Electronics*, vol. 10, no. 15, p. 1826, 2021, https://doi.org/10.3390/electronics10151826.

[33] H. Li, X. Wang, and J. Xiao, "Differential evolution-based load frequency robust control for micro-grids with energy storage systems," *Energies*, vol. 11, no. 7, p. 1686, 2018,

https://doi.org/10.3390/en11071686.

[34] H. M. Hasanien, “Transient Stability Augmentation of a Wave Energy Conversion System Using a Water Cycle Algorithm-Based Multiobjective Optimal Control Strategy,” *IEEE Transactions on Industrial Informatics*, vol. 15, no. 6, pp. 3411-3419, 2019, https://doi.org/10.1109/TII.2018.2871098.

[35] P. Purey and R. Arya, “Application of Jaya Algorithm for reactive power reserve optimization accounting constraints on voltage stability margin,” *International Journal of Engineering Trends and Technology*, vol. 51, no. 2, pp. 106-114, 2017, https://doi.org/10.14445/22315381/IJETT-V51P219.

[36] S. Vachirasricirikul and I. Ngamroo, “Robust controller design of heat pump and plug-in hybrid electric vehicle for frequency control in a smart microgrid based on specified-structure mixed H2/H∞ control technique,” *Applied Energy*, vol. 88, no. 11, pp. 3860-3868, 2011, https://doi.org/10.1016/j.apenergy.2011.04.055.

[37] R. Ali, T. H. Mohamed, Y. S. Qudaih, and Y. Mitani, “A new load frequency control approach in an isolated small power systems using coefficient diagram method,” *International Journal of Electrical Power & Energy Systems*, vol. 56, pp. 110-116, 2014, https://doi.org/10.1016/j.ijepes.2013.11.002.

[38] I. A. Khan, H. Mokhlis, N. N. Mansor, H. A. Illias, L. Jamilatul Awalin, and L. Wang, “New trends and future directions in load frequency control and flexible power system: A comprehensive review,” *Alexandria Engineering Journal*, vol. 71, pp. 263-308, 2023, https://doi.org/10.1016/j.aej.2023.03.040.

[39] G. I. Sayed, A. Darwish, and A. E. Hassanien, “A New Chaotic Whale Optimization Algorithm for Features Selection,” *Journal of Classification*, vol. 35, pp. 300-344, 2018, https://doi.org/10.1007/s00357-018-9261-2.

[40] C. Andic, S. Ozumcan, M. Varan, and A. Ozturk, “A Novel Sea Horse Optimizer Based Load Frequency Controller for Two-Area Power System with PV and Thermal Units,” *International Journal of Robotics and Control Systems*, vol. 4, no. 2, pp. 606-627, 2023, https://doi.org/10.31763/ijrcs.v4i2.1341.

[41] H. Nenavath and R. K. Jatoth, “Hybridizing sine cosine algorithm with differential evolution for global optimization and object tracking,” *Applied Soft Computing*, vol. 62, pp. 1019-1043, 2018, https://doi.org/10.1016/j.asoc.2017.09.039.

[42] Y. Wan, A. Ma, Y. Zhong, X. Hu and L. Zhang, “Multiobjective Hyperspectral Feature Selection Based on Discrete Sine Cosine Algorithm,” *IEEE Transactions on Geoscience and Remote Sensing*, vol. 58, no. 5, pp. 3601-3618, 2020, https://doi.org/10.1109/TGRS.2019.2958812.

[43] W. Long, T. Wu, X. Liang, and S. Xu, “Solving high-dimensional global optimization problems using an improved sine cosine algorithm,” *Expert Systems with Applications*, vol. 123, pp. 108-126, 2019, https://doi.org/10.1016/j.eswa.2018.11.032.

[44] W. Long, J. Jiao, X. Liang, S. Cai and M. Xu, “A Random Opposition-Based Learning Grey Wolf Optimizer,” *IEEE Access*, vol. 7, pp. 113810-113825, 2019, https://doi.org/10.1109/ACCESS.2019.2934994.

[45] T. H. Mohamed, H. Abubakr, M. A. M. Alamin and A. M. Hassan, “Modified WCA-Based Adaptive Control Approach Using Balloon Effect: Electrical Systems Applications,” *IEEE Access*, vol. 8, pp. 60877-60889, 2020, https://doi.org/10.1109/ACCESS.2020.2982510.

[46] M. I. A. E. Ali, A. A. Z. Diab and A. A. Hassan, “Adaptive Load Frequency Control Based on Dynamic Jaya Optimization Algorithm of Power System with Renewable Energy Integration,” *2019 21st International Middle East Power Systems Conference (MEPCON)*, pp. 202-206, 2019, https://doi.org/10.1109/MEPCON47431.2019.9007955.

[47] T. Hassan Mohamed and M. M. Hussein, “Online Gain Tuning of Conventional Load Frequency Controller for Microgrid Power System,” *2018 Twentieth International Middle East Power Systems Conference (MEPCON)*, pp. 424-428, 2018, https://doi.org/10.1109/MEPCON.2018.8635107.